
Enhancing Multimodal Large Language Models with Vision Detection Models: An Empirical Study

Qirui Jiao

Sun Yat-Sen University
jiaoqr3@mail2.sysu.edu.cn

Daoyuan Chen

Alibaba Group
daoyuanchen.cdy@alibaba-inc.com

Yilun Huang

Alibaba Group
lielin.hyl@alibaba-inc.com

Yaliang Li

Alibaba Group
yaliang.li@alibaba-inc.com

Ying Shen

Sun Yat-Sen University
sheny76@mail.sysu.edu.cn

Abstract

Despite the impressive capabilities of Multimodal Large Language Models (MLLMs) in integrating text and image modalities, challenges remain in accurately interpreting detailed visual elements. This paper presents an empirical study on enhancing MLLMs with state-of-the-art (SOTA) object detection and Optical Character Recognition (OCR) models to improve fine-grained understanding and reduce hallucination in responses. We investigate the embedding-based infusion of textual detection information, the impact of such infusion on MLLMs' original abilities, and the interchangeability of detection models. We conduct systematic and extensive experiments with representative models such as LLaVA-1.5, DINO, PaddleOCRv2, and Grounding DINO, revealing that our simple yet general approach not only refines MLLMs' performance in fine-grained visual tasks but also maintains their original strengths. Notably, the enhanced LLaVA-1.5 outperforms its original 7B/13B models on all 10 benchmarks, achieving an improvement of up to 12.5% on the normalized average score. We release our codes to facilitate further exploration into the fine-grained multimodal capabilities of MLLMs.

1 Introduction

The advent of large language models (LLMs) has marked a new epoch in natural language processing [3, 47], laying the groundwork for the evolution of Multimodal Large Language Models (MLLMs) that blend linguistic and visual understanding. Pioneers such as GPT4V have led the charge, showcasing remarkable proficiency in numerous tasks [53]. Despite their successes, a gap remains in these models' ability to discern and accurately respond to queries about fine details within images [12]. This shortfall is particularly evident when MLLMs generate responses that are coherent yet misaligned with the image content, a phenomenon often referred to as "hallucination" [26, 16].

Drawing parallels to human communication, where specificity in referencing objects is key to clarity, MLLMs stand to gain from improved precision in identifying objects and texts within images. To this end, one promising yet under-explored research direction is to leverage state-of-the-art (SOTA) object detection and Optical Character Recognition (OCR) technologies to alleviate hallucination.

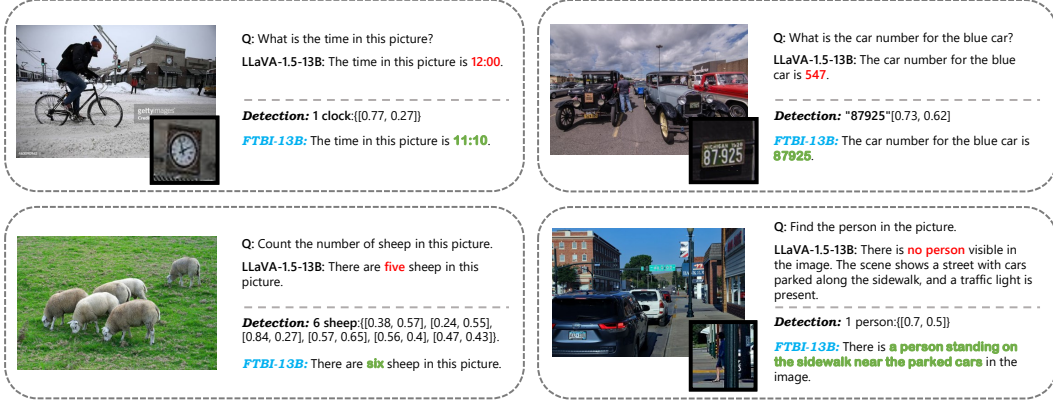


Figure 1: Examples on which LLaVA-1.5-13B fails while our model with detection information (FTBI-13B) succeeds. “Detection” indicates processed detection information from OD/OCR models. More examples are provided in Figure 5 of Appendix A.1.

The prowess of contemporary object detection and OCR models in precisely delineating objects and texts within images is well-established [62, 34]. In this paper, we hypothesize that their outputs can serve as the foundation for improving MLLMs’ fine-grained understanding of images, and investigate how to effectively infuse this information. Based on the experimental analysis of representative SOTA models including LLaVA-1.5 [30], DINO [59], PaddleOCRv2 [11] and Grounding DINO [32] in the main page, as well as the experimental analysis of Qwen-VL [2] and YOLOv8 [20] in the Appendix, we systematically address the following issues:

(1) What if we directly input detection information into MLLMs? A straightforward method to enhance MLLMs with detection information is to feed the textual representation of detected targets directly into the model without additional training, leveraging the pre-existing language understanding abilities of the original MLLM. Our empirical study first focuses on this approach. Interestingly, the results reveal that while the 7B variant of LLaVA-1.5 shows modest gains, the 13B variant deteriorates, underscoring the need for additional model training.

(2) Does training with detection information harm MLLM’s original ability? As applying in-context learning on MLLMs results in excessively long input sequences, we opt to employ a training-based methodology to instruct the model in the recognition of detection information instead. We empirically show that retraining LLaVA-1.5 with detection information enhances its ability to understand detection results, yet dependency on this new information can overshadow MLLM’s original ability to leverage ViT [10] features, resulting in a decline in MLLM’s abilities outside of fine-grained understanding. Then, we further explore suitable fine-tuning strategies and show how to effectively harmonize these impacted abilities.

(3) What if we replace the detection models? The characteristics and performance of leveraged detection models impact the effectiveness of the enhanced MLLM. We examine the replacement of DINO with an open-set object detection model called GroundingDINO [32]. The result shows further enhancement on the MLLM, with new capabilities to dynamically align object detection with the context of user queries during inference. The result also underscores the robustness of the studied infusion approach, as the enhanced MLLM remains functional and effective following the replacement of detection models, leaving great potential for future stronger detection models.

As a result, our experiments affirm the value of detection model infusion and provide several practical insights, with our enhanced LLaVA-1.5 significantly outperforming its original models across all 10 benchmarks, making a notable improvement in multimodal understanding. As shown in Figure 1, the enhanced model effectively reduces hallucination and showcases enhanced efficacy in counting and localization tasks. For OCR tasks, it can also produce more accurate responses.

Our contributions can be summarized as follows:

- We conduct a thorough empirical investigation for the integration of both object detection and OCR models into an MLLM, with a particular focus on infusion strategies. Furthermore,

we explore the replacement of an open-set detector to enable question-driven detection and validate the sustained efficacy of our method following the substitution of detection models.

- Built upon the insights gained, we develop a simple yet general approach for fine-grained image understanding, which elevates LLaVA-1.5 with 12.5% and 11.5% overall improvements for 7B and 13B size respectively, across 10 comprehensive MLLM benchmarks.
- Our code is publicly available at *anonymous link* to facilitate further research, which we hope to help pave the way for systems that engage in more nuanced and accurate multimodal dialogue.

2 Related Works

2.1 Multimodal Large Language Models (MLLMs)

Large Language Models (LLMs) are primarily tailored for text-based tasks [61]. To integrate visual information, modality bridging modules have been developed to reconcile the representational disparities between text and images [55]. Commonly, there are three kinds of them:

Firstly, learnable queries are used to distill information from image features. For example, Flamingo’s [1] perceiver resampler and IDEFICS’s [19, 24] similar modules employ learnable queries to extract ViT features. BLIP-2 [27] uses learnable queries in conjunction with a Q-Former module, while Qwen-VL [2] compresses visual features into a sequence of fixed length using a cross-attention layer. Secondly, projection-based interfaces are employed to bridge modalities. Noteworthy models like LLaVA [31] and LLaVA-1.5 [30] use simple linear layers for mapping image features into the text semantic space. Lastly, parameter-efficient tuning modules are used. LLaMA-Adapter [60, 13] introduces self-attention layers with zero gating, and LaVIN [37] employs modality-specific adapters.

In the main page, we present experimental results for LLaVA-1.5 because its architecture aligns with the majority of current SOTA MLLMs, making it an appropriate representation. More detailed discussion and empirical support are provided in Appendix D.1, where we also conduct experiments on another MLLM, Qwen-VL, and obtain results with similar trends to verify our conclusions.

2.2 Enhancing Detection Capabilities for MLLMs

For models designed for image tasks, the ability to detect and localize targets is crucial. To improve MLLMs’ detection capabilities, typically three categories of methods are explored:

The first category is to expand the dataset with existing object detection or OCR data. InstructBLIP [8] uses data from 26 datasets spanning 11 tasks, including OCR data. Shikra [6] integrates object detection dataset RefCOCO [21] and PointQA [38], and generates more related data with GPT-4 and Flickr30K [42]. ASM [48] introduces 1B region-text pairs. LLaVA and SPHINX [29] compile hybrid instruction fine-tuning datasets including object detection dataset RefCOCO, VG [22], and OCR dataset OCRVQA [40]. PINK [52] employs a bootstrapping method to cover a range of referential comprehension datasets.

The second category is to restructure the image encoder to extract fine-grained features. LION [5] introduces a module called Vision Aggregator for feature aggregation. Honeybee [4] uses a deformable attention-based abstractor with initialized reference points for fine-grained detail capture. UReader [54] employs a shape-adaptive cropping module and learnable queries to process local image features. Vary [51] develops a dedicated image encoder for text recognition. Although these approaches can enhance the detection capabilities of MLLMs, they usually require a considerable volume of data to train the supplementary modules.

The third category is to introduce detection models into MLLMs’ output end to train MLLMs or perform detection tasks. UNIFIED-IO [36, 35] unifies image, text, and detection features into discrete tokens and trains an end-to-end MLLM capable of detecting. ContextDET [57] trains a visual decoder for predicting bounding boxes with contextual LLM tokens. Lenna [50], Lisa [23], and Next-chat [58] introduce an additional token to prompt the detector to identify targets. Similar to the second category, these approaches also require a substantial amount of data to achieve feature alignment.

Distinct from them, we opt not to expand datasets or introduce new architectures. Instead, we use the same datasets and architectures of the target MLLM to be infused, and employ off-the-shelf detection

models to infuse textual detection information into the input end of the MLLM. Doing so allows MLLMs to achieve strong performance with minimal training effort as shown in our experiments.

3 Investigation Methodology for Detection Models Infusion

3.1 Motivational Observation

Existing MLLMs often encounter difficulties in accurately detecting targets. Consider LLaVA-1.5 as an example; despite its exceptional performance across various vision-language tasks, it’s not infallible. As shown in Figure 1, LLaVA-1.5 miscounts a herd of sheep, which points to a limitation in its object-counting capability. Besides, LLaVA-1.5 fails to detect a pedestrian on the street who is partially obscured by a utility pole, underscoring a weakness in its object localization proficiency. In another scenario, LLaVA-1.5 incorrectly recognizes the license plate number “87025” as “547”, revealing a shortcoming in its text recognition functionality.

By contrast, SOTA object detection and OCR models demonstrate superior performance in these tasks. As depicted in Figure 1, detection models yield precise “Detection” annotations. Motivated by the limitations of current MLLMs, we aim to explore the infusion of off-the-shelf detection models into MLLMs. The following section details our empirical investigation into effective fusion strategies.

3.2 Studied Model Architecture

Text-Based Detection Information Construction. With object detection models, we can extract information about the class label and bounding box coordinates of identified objects. We present results for a popular and advanced model, DINO [59], on the main page as a representative. Specifically, we first convert the outputs of DINO into text. To reduce the sentence length, we select the first two values from the bounding box coordinates as positional information, which represent the central coordinates of the corresponding objects. Then, we consolidate objects within the same category, further reducing the length while serving as a counter as well. Finally, we add an instruction sentence before the categories and coordinates information to create the final sentence, whose example looks like: “Here are the central coordinates of certain objects in this image: 2 people:[0.25, 0.12], [0.11, 0.43]}, 1 cake:[0.42, 0.32]}.”

With OCR models, we can extract textual content within images along with their corresponding positional information. In the main page, we adopt PaddleOCRv2 [11] as a representative, a lightweight SOTA OCR system. Similar to object detection, we extract the textual content and corresponding central coordinates from OCR results, process it into text form, and then prepend an instruction sentence to obtain the final sentence, e.g., “Here are the central coordinates of certain texts in this image: ‘Birthday’[0.41, 0.85], ‘YEARS’[0.11, 0.34].”

Specific examples with more images are provided in Appendix A.2. Besides, in Appendix B.1, we conduct statistical analyses on the length of extracted texts, showing that this simple-to-implement constructing method effectively expresses useful information as well as compress the length.

The MLLM Architecture. Figure 2 illustrates the overall architecture of our studied models in different settings, taking the LLaVA-1.5 as an example of the target MLLM to be infused. Firstly, the CLIP-ViT-L-336px [43] is used to extract image-level features and a two-layer MLP is employed to map these features into the text semantic space. Subsequently, we separately use DINO and PaddleOCRv2 to obtain object detection and OCR results. These results are then transformed into sentences using the methods mentioned above and converted into text features using the embedding layers of the backbone LLM. Next, we concatenate the image-level features and the detection features before feeding them into the backbone LLM. As a result, the MLLM can simultaneously obtain both the overall image information and the fine-grained image details during training and inference.

3.3 Studied Infusion Strategies

Besides the model architecture, the training strategy plays a vital role in the detection model infusion. We design a series of experiments to identify effective fusion strategies in terms of model training as follows. We provide a concise introduction here and more implementation details in Appendix B.

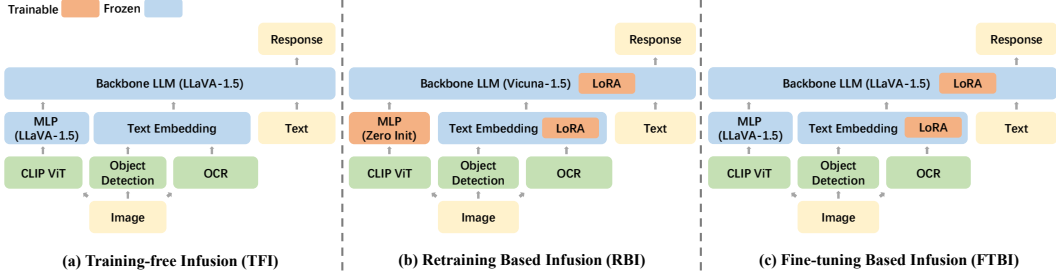


Figure 2: The illustration of investigated MLLM architectures with different strategies to infuse detection information. “(LLaVA-1.5)” denotes module initialization with weights from LLaVA-1.5.

Training-free Infusion (TFI) For the first fusion strategy, we directly feed the detection information into the target MLLM (LLaVA-1.5 here) without any additional training. As shown in Figure 2(a), we use the same model structure and parameter as the target MLLM, with the only distinction being the supplementary input of our detection information (described in Section 3.2).

Retraining Based Infusion (RBI) For the second fusion strategy, we train our model from scratch using the target MLLM’s training pipeline. As shown in Figure 2(b), we first initialize the MLP module and pretrain it with the LCS-558K datasets [30]. Subsequently, we introduce LoRA [15] modules into the backbone LLM, Vicuna-1.5 [7]. After that, we train the LoRA modules and the MLP module during the instruction fine-tuning process with the target MLLM’s original instruction-following dataset, whose details are provided in Appendix B.2. Throughout the entire training process, we continuously infuse the detection information.

Fine-tuning Based Infusion (FTBI) For the third fusion strategy, we conduct fine-tuning on the target MLLM. As shown in Figure 2(c), we freeze the weights of both the MLP module and backbone LLM of the target MLLM. Following this, we introduce LoRA modules to the LLM and train the LoRA module for a single epoch with the target MLLM’s original instruction-following dataset, concurrently infusing the detection information.

3.4 Quantitative Evaluation Settings

We employ 10 benchmarks to evaluate different MLLM capabilities in the main page: VQAv2 [14], GQA [18], and MME [12] measure **comprehensive VQA capabilities**; MMBench [33] and SEED-Bench [25] evaluate **perceptual and reasoning abilities**; TextVQA [46] assesses **text recognition abilities**; MM-Vet [56] evaluates **abilities for managing complex task with local information**; and POPE [28] measures **fine-grained object localization abilities**. Regarding the GQA benchmark, which tends to under-estimate performance due to its textual exact match evaluation setting, we utilize a subset that retains unambiguous questions, denoted as **GQA***. Detailed information of the GQA* is provided in Appendix E.1.

For a more comprehensive and convenient comparison, we employ an aggregated score across all considered benchmarks. Specifically, we first normalize the score for each benchmark as $s_{norm} = (s - s_{min}) / (s_{max} - s_{min})$, where s denotes the original benchmark score, s_{min} and s_{max} refers to the lowest and highest score across all considered methods respectively. Subsequently, we compute the mean of s_{norm} across all benchmarks and denote it as \bar{s}_{norm} .

Benchmark names are abbreviated due to space limits: VQA^{v2} as VQA-v2, VQA^T as TextVQA, MMB as MMBench, MMB^{CN} as MMBench-Chinese, SEED as SEED-Bench, MME^P as MME-Perception, and MME^C as MME-Cognition.

4 Main Results and Analysis

4.1 Lesson 1: Original MLLMs Struggle with Comprehending Detection Information

Initially, we directly feed the detection information into the original LLaVA-1.5, aiming to observe whether the original LLaVA-1.5 can comprehend the detection information we input. We call this fusion strategy “Training-free Infusion” (TFI) as introduced in Section 3.3.

Table 1: Comparison between “Training-free Infusion” (TFI) models and LLaVA-1.5.

MLLM	VQA ^{v2}	GQA*	VQA ^T	POPE	MME ^P	MME ^C	MMB	MMB ^{CN}	MM-Vet	SEED
LLaVA-1.5-7B	78.5	79.6	58.2	85.9	1510.7	355.7	64.3	58.3	30.5	58.6
TFI-7B	78.5	79.2 ↓	59.2 ↑	89.9 ↑	1497.0 ↓	401.0 ↑	65.0 ↑	57.2 ↓	33.7 ↑	60.6 ↑
LLaVA-1.5-13B	80.0	81.0	61.3	85.9	1531.3	295.4	67.7	63.6	35.4	61.6
TFI-13B	76.6 ↓	79.0 ↓	59.6 ↓	88.3 ↑	1453.6 ↓	401.0 ↑	65.0 ↓	57.5 ↓	31.7 ↓	60.7 ↓

Performance Improvement on OD/OCR Tasks. The results are presented in Table 1. We can see that *TFI-7B* exhibits partial enhancement in some benchmarks, while *TFI-13B* shows a discernible decline. Both models show significant improvement on the POPE benchmark, which evaluates object hallucination, indicating that the infused object detection information is helpful for object detection tasks. Additionally, they exhibit robust performance on the MME-Cognition benchmark, which contains numerous questions related to text within images, suggesting that the OCR information is also demonstrating efficacy.

Performance Degradation on Other Tasks. However, other benchmarks exhibit fluctuations in scores, implying a deficiency in our model’s utilization of detection information. Upon closer analysis, we believe that the infusion of detection information introduces extraneous content, which becomes noise, thereby adversely affecting the inference accuracy. Therefore, we proceed to train the model to help it better extract useful information from the detection information and eliminate noise.

4.2 Lesson 2: Detection Re-Training has Adverse Effects on Comprehending ViT Features

Researchers commonly employ in-context learning (ICL) [9] to instruct LLMs in the recognition of specific input formats. However, for MLLMs, ICL becomes difficult as it requires MLLMs to process lengthy input sequences combining image features in tokens format. Therefore, we opt against using ICL for MLLMs in favor of a training-based approach, and shifting into the second fusion strategy introduced in Section 3.3, “Retraining Based Infusion” (RBI). In this strategy, we retrain LLaVA-1.5 with its original training pipeline, concurrently infusing the detection information.

Table 2: Comparison between “Retraining Based Infusion” (RBI) models and LLaVA-1.5.

MLLM	VQA ^{v2}	GQA*	VQA ^T	POPE	MME ^P	MME ^C	MMB	MMB ^{CN}	MM-Vet	SEED
LLaVA-1.5-7B	78.5	79.6	58.2	85.9	1510.7	355.7	64.3	58.3	30.5	58.6
RBI-7B	78.5	76.6 ↓	60.0 ↑	89.3 ↑	1454.5 ↓	412.0 ↑	66.2 ↑	60.6 ↑	31.5 ↑	60.8 ↑
LLaVA-1.5-13B	80.0	81.0	61.3	85.9	1531.3	295.4	67.7	63.6	35.4	61.6
RBI-13B	79.2 ↓	78.0 ↓	61.7 ↑	89.2 ↑	1491.2 ↓	409.6 ↑	69.5 ↑	63.2 ↓	35.1 ↓	62.5 ↑

Table 3: Performance of RBI models without detection information during inference(w/o DI).

MLLM	VQA ^{v2}	GQA*	VQA ^T	POPE	MME ^P	MME ^C	MMB	MMB ^{CN}	MM-Vet	SEED
LLaVA-1.5-7B	78.5	79.6	58.2	85.9	1510.7	355.7	64.3	58.3	30.5	58.6
RBI-7B w/o DI	76.4 ↓	74.8 ↓	56.6 ↓	85.5 ↓	1387.7 ↓	312.5 ↓	65.5 ↑	58.3	29.0 ↓	59.6 ↑
LLaVA-1.5-13B	80.0	81.0	61.3	85.9	1531.3	295.4	67.7	63.6	35.4	61.6
RBI-13B w/o DI	77.3 ↓	76.0 ↓	58.2 ↓	83.4 ↓	1442.6 ↓	310.7 ↑	68.5 ↑	61.7 ↓	30.6 ↓	61.6 ↑

Performance Improvement Relative to LLaVA-1.5 and TFI. As shown in Table 2, *RBI models* excel beyond *LLaVA-1.5* across several benchmarks, particularly the 7B variant. Notably, they outshine on comprehensive benchmarks, MMBench and Seed-Bench, and show a 4% improvement on the POPE benchmark, which assesses object hallucination. Notable gains are also seen in MME-Cognition and TextVQA, which are related to text recognition.

Adverse Impact of RBI on ViT Feature Comprehension. *RBI models* do not show improvement across all benchmarks. On VQA^{v2}, GQA*, and MME, there is a noticeable decline. We speculate that the unexpected results are due to an over-infusion that negatively affects the model’s ability to learn how to utilize features from ViT. Thus, we then evaluate the performance of RBI models with no detection information applied. In this way, their benchmark scores are only related to ViT

Table 4: Comparison between “Retraining Based Infusion” (RBI) models, “Fine-tuning Based Infusion” (FTBI) models, and SOTA methods on 10 benchmarks. Our FTBI approach effectively infuses detection information into LLaVA-1.5, leading to a considerable performance enhancement across all 10 benchmarks. \bar{s}_{norm} is an aggregated performance measure across all considered benchmarks. **Bold** and underlined results indicate the best and second-best performance respectively. MME represents the summation of MME^P and MME^C , with detailed information in Appendix E.2.

MLLM	VQA ^{v2}	GQA*	VQA ^T	POPE	MME	MMB	MMB ^{CN}	MM-Vet	SEED	\bar{s}_{norm}
BLIP-2 (13B)	41.0	41.0	42.5	85.3	1583.8	-	-	22.4	46.4	-
InstructBLIP (13B)	75.3	64.3	50.7	78.9	1504.6	34.5	15.5	25.6	43.6	0.245
Qwen-VL (7B)	78.8	74.8	63.8	78.1	1667.0	38.2	7.4	38.2	56.3	0.512
Qwen-VL-Chat (7B)	78.2	77.9	61.5	79.2	1848.2	60.6	56.7	41.5	58.2	0.756
SPHINX (13B)	78.1	80.4	51.6	80.7	1798.3	66.9	56.2	36.0	69.1	0.746
LLaVA-1.5-7B	78.5	79.6	58.2	85.9	1866.4	64.3	58.3	30.5	58.6	0.767
RBI-7B (our)	78.5	76.6 ↓	60.0 ↑	89.3 ↑	1866.5 ↑	66.2 ↑	60.6 ↑	31.5 ↑	60.8 ↑	0.828 ↑
FTBI-7B (our)	79.0 ↑	80.1 ↑	60.1 ↑	88.9 ↑	1880.5 ↑	67.3 ↑	60.2 ↑	35.2 ↑	60.8 ↑	0.863 ↑
LLaVA-1.5-13B	<u>80.0</u>	<u>81.0</u>	61.3	85.9	1826.7	67.7	63.6	35.4	61.6	0.843
RBI-13B (our)	79.2 ↓	78.0 ↓	61.7 ↑	89.2 ↑	1900.9 ↑	69.5 ↑	63.2 ↓	35.1 ↓	62.5 ↑	0.894 ↑
FTBI-13B (our)	80.3 ↑	81.8 ↑	61.8 ↑	88.8 ↑	1920.5 ↑	71.4 ↑	65.2 ↑	38.9 ↑	62.3 ↑	0.940 ↑

features. As shown in Table 3, the current models show a noticeable performance lag compared to LLaVA-1.5, suggesting that *RBI strategy does impact the MLLM in learning how to use the image features extracted from ViT, calling for further improved fusion strategies.*

4.3 Lesson 3: Suitable Fine-tuning Achieves Good Trade-off for Detection Infusion

To enhance the model’s ability to make well-informed trade-offs between ViT features and detection information, for the third fusion strategy, we leverage the well-trained parameters of LLaVA-1.5 and fine-tune our models based on it. We call this fusion strategy “Fine-tuning Based Infusion”, abbreviated as **FTBI**.

Performance Improvement Relative to LLaVA-1.5 and RBI. As shown in Table 4, *both the 7B and 13B models of FTBI exhibit superior performance compared to LLaVA-1.5.* Simultaneously, as indicated in Appendix C.2, when detection information is not infused, FTBI models demonstrate significant improvement in comparison to the RBI models, indicating that *the fine-tuning strategy effectively makes trade-offs between ViT features and detection information.*

Performance Improvement on All Tasks. Upon detailed analysis, we find that FTBI models exhibit a visible improvement on comprehensive VQA benchmarks such as VQA^{v2}, GQA*, and MME. On the benchmarks that evaluate perceptual and reasoning abilities, such as MMBench and SEED-Bench, the models’ performance undergoes a noticeable enhancement. Moreover, the infusion of object detection information significantly improves performance on both the POPE benchmark, which evaluates object hallucinations, and the MM-Vet benchmark, which measures the ability to utilize local information. Due to the infusion of OCR information, the models also exhibit commendable performance on text-related benchmarks such as TextVQA and MME-cognition. Finally, on the aggregated performance measure \bar{s}_{norm} , FTBI models significantly outperform LLaVA-1.5 and other considered SOTA models, highlighting the substantial effectiveness of our approach.

Case Study. In Figure 1, we list examples on which LLaVA-1.5 produces incorrect answers while our model yields correct responses (more examples are presented in Appendix A.1). With object detection, our model effectively achieves precise counts and delineates the respective positions of specified objects. With OCR, our model proficiently generates textual content in response to the localization requirements. Furthermore, our model can use the object detection information to refine its comprehension of the information conveyed by particular objects. For instance, when the model discerns the location of a clock within the image, it can more effectively extract the displayed content on the clock, thereby acquiring the correct time.

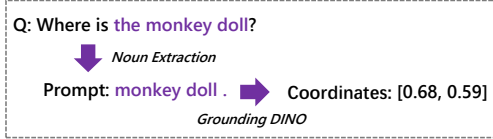


Figure 3: An example of detecting open-set targets with Grounding DINO.

Table 5: Comparison between TFI-7B and FTBI-7B employed Grounding DINO.

	w/ Grounding DINO (box threshold 0.35)				
	VQA ^{v2}	GQA*	POPE	MM-Vet	SEED
TFI-7B	74.1	72.3	73.5	30.9	57.4
FTBI-7B	76.3	77.4	84.6	31.2	59.9



Figure 4: Examples on which LLaVA-1.5 fails while our model with open-set object detection information succeeds.

4.4 Lesson 4: Detection Models Can be Flexibly and Effectively Replaced

DINO is a closed-set object detection model and cannot deal with images containing uncommon objects or specific entities such as certain celebrities and objects with attributive modifiers. Fortunately, our model is modular, which means that we have the flexibility to replace the embedded detection models. Additionally, the modular structure allows our model to retain the training effectiveness of comprehending specially designed detection information after the module replacement.

Constructing Detection Information with Grounding DINO. In this experiment, we will substitute the embedded closed-set detection model DINO with an open-set object detection model called Grounding DINO [32]. Grounding DINO is designed to detect objects related to user-input. With this model, our model can pinpoint the targets by referencing the object names mentioned in questions. To achieve this, we first extract target names from the input questions, and then combine them to create prompts. Grounding DINO then follows the prompts to generate location information for the targets. Finally, we convert the outputs into the specially designed detection information.

Training Effect Inherited Following Replacement of Detection Model. In Table 5, we compare the performance of TFI-7B and FTBI-7B after replacing the detection model DINO with Grounding DINO. We use VQA^{v2}, GQA*, POPE, MM-Vet, and SEED-Bench for evaluation as they contain questions from which effective noun phrases can be extracted. Due to the low detection accuracy of Grounding DINO, some noise is introduced, which results in lower evaluation scores for both models compared to LLaVA-1.5-7B. However, because *FTBI-7B has been trained with DINO and it can filter out some noise*, the performance of FTBI-7B is superior to that of TFI-7B. These results validate that the training effectiveness remains after we replace the detection model.

Case Study. In Figure 4, we enumerate cases where LLaVA-1.5 provides incorrect answers while our model with open-set object detection information produces correct responses. Although Grounding DINO may output error messages, when its outputs are correct, this information can effectively assist our model. With open-set object detection information, our model can carry out counting tasks and localization tasks *more purposefully*, as it can leverage the target names in questions to get specific positional information.

4.5 Overview of More Experiments

Further Experiments and Analysis on the FTBI Models. In Appendix C.1, we fine-tune LLaVA-1.5 without the infusion of detection information and discover that the exceptional performance of FTBI models is primarily ascribed to the infused detection information, rather than the additional fine-tuning. In Appendix C.2, we assess the performance of FTBI models without infusing any detection information, affirming that the FTBI strategy proficiently harnesses ViT features. In Appendix C.3, we show the model’s performance on solely leveraging object detection information and OCR information separately. In Appendix C.4, we assess our models’ inference efficiency, showing that even with the detection infusion, our approach remains efficient with potential for further efficiency gains through modular replacement and text compression strategies.

Model Architecture Rationale. In Appendix D.1, we discuss how does LLaVA-1.5 represents the majority of advanced MLLMs, supported by their architecture alignment and more empirical results on another MLLM, Qwen-VL. In Appendix D.2, we demonstrate the representativeness of DINO and PaddleOCRv2 to other models, thanks to the proposed flexible format that allows us to process the outputs of any detection models into detection information. Besides, we replace DINO with another detector, YOLOv8 [20], yielding similar experimental findings. In Appendix D.3, we show that using text as a bridge to feed detection information into LLMs generally gain superior results without the need for additional data, compared with feeding methods based on MLP or cross-attention training.

Model Performance and Additional Evaluation Benchmarks. In Appendix E.1, we elaborate on the motivations and modifications behind the GQA* from the original GQA benchmark. In Appendix E.2, we present detailed MME benchmark scores. In Appendix E.3, we evaluate our model’s ability to ground specific linguistic phenomena with the VALSE benchmark [41]. In Appendix E.4, we explore the variants of calculation of aggregated score \bar{s}_{norm} , based on importance weights of benchmarks.

4.6 Limitation and Future Work

Refinement of Detection Models. The success of our model relies heavily on the accuracy and reliability of the incorporated detection models. However, existing detection models are not flawless, as they still make mistakes when encountering challenging issues. For instance, our model’s improvement on the TextVQA benchmark is not very significant, primarily due to TextVQA being a scene-text dataset, and PaddleOCRv2 performs poorly on such data. Fortunately, both object detection and OCR models are still rapidly advancing [62]. It’s believed that highly accurate and fast models will emerge in the near future. Therefore, future work could explore the development and infusion of more advanced detection models to further improve the MLLMs.

Extended Token Sequences. The infusion of detection information into token sequences extends the typical input length for the backbone LLM, potentially impacting inference speed negatively. Nonetheless, our statistical investigation reveals that the detection data, thanks to compressed prompts, mostly remain succinct. Furthermore, advancements in AI hardware, particularly the rapid evolution of AI chips, coupled with ongoing research efforts to expand the contextual capacity of LLMs [17], are progressively alleviating the imposed constraints. Future work could upgrade our MLLMs to support LLMs with longer contextual windows, further enhancing the performance.

5 Conclusion

In this paper, we systematically conduct substantial experiments to find effective strategies for incorporating SOTA object detection and OCR models into MLLMs. We validate the effectiveness of leveraging text as an intermediary to infuse detection information. After thorough investigation, we determine that fine-tuning the original MLLM for an additional epoch, along with the simultaneous infusion of detection information, proves to be the most effective approach compared to the training-free strategy and retraining strategy. Moreover, we replace the detection model from DINO to GroundingDINO and observe that the updated model continues to function properly and retains the training effect. This highlights the modular structure of our model, demonstrating its capability to stay abreast of evolving object detection technologies and gain sustained performance enhancement.

We offer guidance on how to infuse detection information into MLLMs. If people want to enhance the zero-initialized MLLMs, they can consider introducing detection modules throughout the training process to achieve effects similar to those of RBI models. To further improve the performance, they can initially train the model without detection information to develop robust non-detail-related capabilities. Then, they can introduce detection modules and fine-tune the model to develop visual grounding capabilities. If people aim to enhance pre-trained MLLMs, they can directly conduct additional fine-tuning on the model while infusing detection information simultaneously.

In a nutshell, we provide a series of progressive insights about the effective incorporation of vision detection models for MLLMs, and derive models that exhibit exceptional performance in various tasks such as counting, object localization, and text recognition. With this work, we hope it can benefit future MLLM research and development that approaches better understanding, interpreting and engaging with fine-grained multimodal content.

References

- [1] Jean-Baptiste Alayrac, Jeff Donahue, Pauline Luc, Antoine Miech, Iain Barr, Yana Hasson, Karel Lenc, Arthur Mensch, Katherine Millican, Malcolm Reynolds, et al. Flamingo: a visual language model for few-shot learning. *Advances in Neural Information Processing Systems*, 35:23716–23736, 2022.
- [2] Jinze Bai, Shuai Bai, Shusheng Yang, Shijie Wang, Sinan Tan, Peng Wang, Junyang Lin, Chang Zhou, and Jingren Zhou. Qwen-vl: A frontier large vision-language model with versatile abilities. *arXiv preprint arXiv:2308.12966*, 2023.
- [3] Tom Brown, Benjamin Mann, Nick Ryder, Melanie Subbiah, Jared D Kaplan, Prafulla Dhariwal, Arvind Neelakantan, Pranav Shyam, Girish Sastry, Amanda Askell, et al. Language models are few-shot learners. *Advances in neural information processing systems*, 33:1877–1901, 2020.
- [4] Junbum Cha, Wooyoung Kang, Jonghwan Mun, and Byungseok Roh. Honeybee: Locality-enhanced projector for multimodal llm. *arXiv preprint arXiv:2312.06742*, 2023.
- [5] Gongwei Chen, Leyang Shen, Rui Shao, Xiang Deng, and Liqiang Nie. Lion: Empowering multimodal large language model with dual-level visual knowledge. *arXiv preprint arXiv:2311.11860*, 2023.
- [6] Keqin Chen, Zhao Zhang, Weili Zeng, Richong Zhang, Feng Zhu, and Rui Zhao. Shikra: Unleashing multimodal llm’s referential dialogue magic. *arXiv preprint arXiv:2306.15195*, 2023.
- [7] Wei-Lin Chiang, Zhuohan Li, Zi Lin, Ying Sheng, Zhanghao Wu, Hao Zhang, Lianmin Zheng, Siyuan Zhuang, Yonghao Zhuang, Joseph E Gonzalez, et al. Vicuna: An open-source chatbot impressing gpt-4 with 90%* chatgpt quality. See <https://vicuna.lmsys.org> (accessed 14 April 2023), 2023.
- [8] W Dai, J Li, D Li, AMH Tiong, J Zhao, W Wang, B Li, P Fung, and S Hoi. Instructblip: Towards general-purpose vision-language models with instruction tuning. *arXiv preprint arXiv:2305.06500*, 2023.
- [9] Qingxiu Dong, Lei Li, Damai Dai, Ce Zheng, Zhiyong Wu, Baobao Chang, Xu Sun, Jingjing Xu, and Zhifang Sui. A survey for in-context learning. *arXiv preprint arXiv:2301.00234*, 2022.
- [10] Alexey Dosovitskiy, Lucas Beyer, Alexander Kolesnikov, Dirk Weissenborn, Xiaohua Zhai, Thomas Unterthiner, Mostafa Dehghani, Matthias Minderer, Georg Heigold, Sylvain Gelly, et al. An image is worth 16x16 words: Transformers for image recognition at scale. *arXiv preprint arXiv:2010.11929*, 2020.
- [11] Yuning Du, Chenxia Li, Ruoyu Guo, Cheng Cui, Weiwei Liu, Jun Zhou, Bin Lu, Yehua Yang, Qiwen Liu, Xiaoguang Hu, et al. Pp-ocrv2: Bag of tricks for ultra lightweight ocr system. *arXiv preprint arXiv:2109.03144*, 2021.
- [12] Chaoyou Fu, Peixian Chen, Yunhang Shen, Yulei Qin, Mengdan Zhang, Xu Lin, Jinrui Yang, Xiawu Zheng, Ke Li, Xing Sun, et al. Mme: A comprehensive evaluation benchmark for multimodal large language models. *arXiv preprint arXiv:2306.13394*, 2023.
- [13] Peng Gao, Jiaming Han, Renrui Zhang, Ziyi Lin, Shijie Geng, Aojun Zhou, Wei Zhang, Pan Lu, Conghui He, Xiangyu Yue, et al. Llama-adapter v2: Parameter-efficient visual instruction model. *arXiv preprint arXiv:2304.15010*, 2023.
- [14] Yash Goyal, Tejas Khot, Douglas Summers-Stay, Dhruv Batra, and Devi Parikh. Making the v in vqa matter: Elevating the role of image understanding in visual question answering. In *Proceedings of the IEEE conference on computer vision and pattern recognition*, pages 6904–6913, 2017.
- [15] Edward J Hu, Yelong Shen, Phillip Wallis, Zeyuan Allen-Zhu, Yuanzhi Li, Shean Wang, Lu Wang, and Weizhu Chen. Lora: Low-rank adaptation of large language models. *arXiv preprint arXiv:2106.09685*, 2021.
- [16] Lei Huang, Weijiang Yu, Weitao Ma, Weihong Zhong, Zhangyin Feng, Haotian Wang, Qianglong Chen, Weihua Peng, Xiaocheng Feng, Bing Qin, et al. A survey on hallucination in large language models: Principles, taxonomy, challenges, and open questions. *arXiv preprint arXiv:2311.05232*, 2023.

- [17] Yunpeng Huang, Jingwei Xu, Junyu Lai, Zixu Jiang, Taolue Chen, Zenan Li, Yuan Yao, Xiaoxing Ma, Lijuan Yang, Hao Chen, Shupeng Li, and Penghao Zhao. Advancing transformer architecture in long-context large language models: A comprehensive survey, 2024.
- [18] Drew A Hudson and Christopher D Manning. Gqa: A new dataset for real-world visual reasoning and compositional question answering. In *Proceedings of the IEEE/CVF conference on computer vision and pattern recognition*, pages 6700–6709, 2019.
- [19] Laurençon Hugo, van Strien Daniel, Bekman Stas, Tronchon Leo, Saulnier Lucile, Wang Thomas, Karamcheti Siddharth, Singh Amanpreet, Pistilli Giada, Jernite Yacine, and Sanh Victor. Introducing idefics: An open reproduction of state-of-the-art visual language model. <https://huggingface.co/blog/idefics>, 2023.
- [20] Glenn Jocher, Ayush Chaurasia, and Jing Qiu. Ultralytics YOLO, January 2023.
- [21] Sahar Kazemzadeh, Vicente Ordonez, Mark Matten, and Tamara Berg. Referitgame: Referring to objects in photographs of natural scenes. In *Proceedings of the 2014 conference on empirical methods in natural language processing (EMNLP)*, pages 787–798, 2014.
- [22] Ranjay Krishna, Yuke Zhu, Oliver Groth, Justin Johnson, Kenji Hata, Joshua Kravitz, Stephanie Chen, Yannis Kalantidis, Li-Jia Li, David A Shamma, et al. Visual genome: Connecting language and vision using crowdsourced dense image annotations. *International journal of computer vision*, 123:32–73, 2017.
- [23] Xin Lai, Zhuotao Tian, Yukang Chen, Yanwei Li, Yuhui Yuan, Shu Liu, and Jiaya Jia. Lisa: Reasoning segmentation via large language model. In *The Twelfth International Conference on Learning Representations*, 2023.
- [24] Hugo Laurençon, Léo Tronchon, Matthieu Cord, and Victor Sanh. What matters when building vision-language models? *arXiv preprint arXiv:2405.02246*, 2024.
- [25] Bohao Li, Rui Wang, Guangzhi Wang, Yuying Ge, Yixiao Ge, and Ying Shan. Seed-bench: Benchmarking multimodal llms with generative comprehension. *arXiv preprint arXiv:2307.16125*, 2023.
- [26] Chunyuan Li, Zhe Gan, Zhengyuan Yang, Jianwei Yang, Linjie Li, Lijuan Wang, and Jianfeng Gao. Multi-modal foundation models: From specialists to general-purpose assistants. *arXiv preprint arXiv:2309.10020*, 1(2):2, 2023.
- [27] Junnan Li, Dongxu Li, Silvio Savarese, and Steven Hoi. Blip-2: Bootstrapping language-image pre-training with frozen image encoders and large language models. *arXiv preprint arXiv:2301.12597*, 2023.
- [28] Yifan Li, Yifan Du, Kun Zhou, Jinpeng Wang, Wayne Xin Zhao, and Ji-Rong Wen. Evaluating object hallucination in large vision-language models. *arXiv preprint arXiv:2305.10355*, 2023.
- [29] Ziyi Lin, Chris Liu, Renrui Zhang, Peng Gao, Longtian Qiu, Han Xiao, Han Qiu, Chen Lin, Wenqi Shao, Keqin Chen, et al. Sphinx: The joint mixing of weights, tasks, and visual embeddings for multi-modal large language models. *arXiv preprint arXiv:2311.07575*, 2023.
- [30] Haotian Liu, Chunyuan Li, Yuheng Li, and Yong Jae Lee. Improved baselines with visual instruction tuning. *arXiv preprint arXiv:2310.03744*, 2023.
- [31] Haotian Liu, Chunyuan Li, Qingyang Wu, and Yong Jae Lee. Visual instruction tuning. *arXiv preprint arXiv:2304.08485*, 2023.
- [32] Shilong Liu, Zhaoyang Zeng, Tianhe Ren, Feng Li, Hao Zhang, Jie Yang, Chunyuan Li, Jianwei Yang, Hang Su, Jun Zhu, et al. Grounding dino: Marrying dino with grounded pre-training for open-set object detection. *arXiv preprint arXiv:2303.05499*, 2023.
- [33] Yuan Liu, Haodong Duan, Yuanhan Zhang, Bo Li, Songyang Zhang, Wangbo Zhao, Yike Yuan, Jiaqi Wang, Conghui He, Ziwei Liu, et al. Mmbench: Is your multi-modal model an all-around player? *arXiv preprint arXiv:2307.06281*, 2023.
- [34] Yuliang Liu, Zhang Li, Biao Yang, Chunyuan Li, Xucheng Yin, Cheng lin Liu, Lianwen Jin, and Xiang Bai. On the hidden mystery of ocr in large multimodal models, 2024.
- [35] Jiasen Lu, Christopher Clark, Sangho Lee, Zichen Zhang, Savya Khosla, Ryan Marten, Derek Hoiem, and Aniruddha Kembhavi. Unified-io 2: Scaling autoregressive multimodal models with vision, language, audio, and action. *arXiv preprint arXiv:2312.17172*, 2023.
- [36] Jiasen Lu, Christopher Clark, Rowan Zellers, Roozbeh Mottaghi, and Aniruddha Kembhavi. Unified-io: A unified model for vision, language, and multi-modal tasks. In *The Eleventh International Conference on Learning Representations*, 2022.
- [37] Gen Luo, Yiyi Zhou, Tianhe Ren, Shengxin Chen, Xiaoshuai Sun, and Rongrong Ji. Cheap and quick: Efficient vision-language instruction tuning for large language models. *arXiv preprint arXiv:2305.15023*, 2023.
- [38] Arjun Mani, Nobline Yoo, Will Hinthorn, and Olga Russakovsky. Point and ask: Incorporating pointing into visual question answering. *arXiv preprint arXiv:2011.13681*, 2020.

- [39] Kenneth Marino, Mohammad Rastegari, Ali Farhadi, and Roozbeh Mottaghi. Ok-vqa: A visual question answering benchmark requiring external knowledge. In *Proceedings of the IEEE/cvf conference on computer vision and pattern recognition*, pages 3195–3204, 2019.
- [40] Anand Mishra, Shashank Shekhar, Ajeet Kumar Singh, and Anirban Chakraborty. Ocr-vqa: Visual question answering by reading text in images. In *2019 international conference on document analysis and recognition (ICDAR)*, pages 947–952. IEEE, 2019.
- [41] Letitia Parcalabescu, Michele Cafagna, Lilitta Muradjan, Anette Frank, Iacer Calixto, and Albert Gatt. Valse: A task-independent benchmark for vision and language models centered on linguistic phenomena. In *Proceedings of the 60th Annual Meeting of the Association for Computational Linguistics (Volume 1: Long Papers)*. Association for Computational Linguistics, 2022.
- [42] Bryan A Plummer, Liwei Wang, Chris M Cervantes, Juan C Caicedo, Julia Hockenmaier, and Svetlana Lazebnik. Flickr30k entities: Collecting region-to-phrase correspondences for richer image-to-sentence models. In *Proceedings of the IEEE international conference on computer vision*, pages 2641–2649, 2015.
- [43] Alec Radford, Jong Wook Kim, Chris Hallacy, Aditya Ramesh, Gabriel Goh, Sandhini Agarwal, Girish Sastry, Amanda Askell, Pamela Mishkin, Jack Clark, et al. Learning transferable visual models from natural language supervision. In *International conference on machine learning*, pages 8748–8763. PMLR, 2021.
- [44] Dustin Schwenk, Apoorv Khandelwal, Christopher Clark, Kenneth Marino, and Roozbeh Mottaghi. A-okvqa: A benchmark for visual question answering using world knowledge. In *European Conference on Computer Vision*, pages 146–162. Springer, 2022.
- [45] Oleksii Sidorov, Ronghang Hu, Marcus Rohrbach, and Amanpreet Singh. Textcaps: a dataset for image captioning with reading comprehension. In *Computer Vision—ECCV 2020: 16th European Conference, Glasgow, UK, August 23–28, 2020, Proceedings, Part II 16*, pages 742–758. Springer, 2020.
- [46] Amanpreet Singh, Vivek Natarajan, Meet Shah, Yu Jiang, Xinlei Chen, Dhruv Batra, Devi Parikh, and Marcus Rohrbach. Towards vqa models that can read. In *Proceedings of the IEEE/CVF conference on computer vision and pattern recognition*, pages 8317–8326, 2019.
- [47] Hugo Touvron, Thibaut Lavril, Gautier Izacard, Xavier Martinet, Marie-Anne Lachaux, Timothée Lacroix, Baptiste Rozière, Naman Goyal, Eric Hambro, Faisal Azhar, et al. Llama: Open and efficient foundation language models. *arXiv preprint arXiv:2302.13971*, 2023.
- [48] Weiyun Wang, Min Shi, Qingyun Li, Wenhai Wang, Zhenhang Huang, Linjie Xing, Zhe Chen, Hao Li, Xizhou Zhu, Zhiguo Cao, et al. The all-seeing project: Towards panoptic visual recognition and understanding of the open world. In *The Twelfth International Conference on Learning Representations*, 2023.
- [49] Yulin Wang, Yizeng Han, Chaofei Wang, Shiji Song, Qi Tian, and Gao Huang. Computation-efficient deep learning for computer vision: A survey, 2023.
- [50] Fei Wei, Xinyu Zhang, Ailing Zhang, Bo Zhang, and Xiangxiang Chu. Lenna: Language enhanced reasoning detection assistant. *arXiv preprint arXiv:2312.02433*, 2023.
- [51] Haoran Wei, Lingyu Kong, Jinyue Chen, Liang Zhao, Zheng Ge, Jinrong Yang, Jianjian Sun, Chunrui Han, and Xiangyu Zhang. Vary: Scaling up the vision vocabulary for large vision-language models. *arXiv preprint arXiv:2312.06109*, 2023.
- [52] Shiyu Xuan, Qingpei Guo, Ming Yang, and Shiliang Zhang. Pink: Unveiling the power of referential comprehension for multi-modal llms. *arXiv preprint arXiv:2310.00582*, 2023.
- [53] Zhengyuan Yang, Linjie Li, Kevin Lin, Jianfeng Wang, Chung-Ching Lin, Zicheng Liu, and Lijuan Wang. The dawn of llms: Preliminary explorations with gpt-4v (ision). *arXiv preprint arXiv:2309.17421*, 9(1):1, 2023.
- [54] Jiabo Ye, Anwen Hu, Haiyang Xu, Qinghao Ye, Ming Yan, Guohai Xu, Chenliang Li, Junfeng Tian, Qi Qian, Ji Zhang, et al. Ureader: Universal ocr-free visually-situated language understanding with multimodal large language model. *arXiv preprint arXiv:2310.05126*, 2023.
- [55] Shukang Yin, Chaoyou Fu, Sirui Zhao, Ke Li, Xing Sun, Tong Xu, and Enhong Chen. A survey on multimodal large language models. *arXiv preprint arXiv:2306.13549*, 2023.
- [56] Weihao Yu, Zhengyuan Yang, Linjie Li, Jianfeng Wang, Kevin Lin, Zicheng Liu, Xinchao Wang, and Lijuan Wang. Mm-vet: Evaluating large multimodal models for integrated capabilities. *arXiv preprint arXiv:2308.02490*, 2023.
- [57] Yuhang Zang, Wei Li, Jun Han, Kaiyang Zhou, and Chen Change Loy. Contextual object detection with multimodal large language models. *arXiv preprint arXiv:2305.18279*, 2023.
- [58] Ao Zhang, Liming Zhao, Chen-Wei Xie, Yun Zheng, Wei Ji, and Tat-Seng Chua. Next-chat: An llm for chat, detection and segmentation. In *ICML*, 2024.

- [59] Hao Zhang, Feng Li, Shilong Liu, Lei Zhang, Hang Su, Jun Zhu, Lionel M Ni, and Heung-Yeung Shum. Dino: Detr with improved denoising anchor boxes for end-to-end object detection. *arXiv preprint arXiv:2203.03605*, 2022.
- [60] Renrui Zhang, Jiaming Han, Aojun Zhou, Xiangfei Hu, Shilin Yan, Pan Lu, Hongsheng Li, Peng Gao, and Yu Qiao. Llama-adapter: Efficient fine-tuning of language models with zero-init attention. *arXiv preprint arXiv:2303.16199*, 2023.
- [61] Wayne Xin Zhao, Kun Zhou, Junyi Li, Tianyi Tang, Xiaolei Wang, Yupeng Hou, Yingqian Min, Beichen Zhang, Junjie Zhang, Zican Dong, Yifan Du, Chen Yang, Yushuo Chen, Zhipeng Chen, Jinhao Jiang, Ruiyang Ren, Yifan Li, Xinyu Tang, Zikang Liu, Peiyu Liu, Jian-Yun Nie, and Ji-Rong Wen. A survey of large language models, 2023.
- [62] Zhengxia Zou, Keyan Chen, Zhenwei Shi, Yuhong Guo, and Jieping Ye. Object detection in 20 years: A survey. *Proceedings of the IEEE*, 111(3):257–276, 2023.

Appendix

We provide more details and experiments of this work in the appendix and organize them as follows:

Appendix A, **More Demonstrative Examples:**

- Appendix A.1: we provide examples on which LLaVA-1.5-13B fails while our model FTBI-13B with detection information succeeds.
- Appendix A.2: we provide examples of images along with their corresponding detection information, showing how the detection information is constructed.

Appendix B, **Implementation Details:**

- Appendix B.1: we conduct a statistical analysis on the length of detection information, showcasing the efficacy of our compression strategy.
- Appendix B.2: we introduce the instruction-following dataset of LLaVA-1.5.
- Appendix B.3: we show the different input resolutions of images across three branches: CLIP-ViT, DINO, and PaddleOCRv2.
- Appendix B.4: we show the thresholds we set for filtering the outputs of detection models.
- Appendix B.5: we list the training hyperparameters of our training strategies.
- Appendix B.6: we show the time consumption required for training models.

Appendix C, **Further Experiments and Analysis on the FTBI Model:**

- Appendix C.1: we fine-tune LLaVA-1.5 without the infusion of detection information and get new models. The results indicate that the exceptional performance of FTBI models is primarily ascribed to the infused detection information, rather than the additional fine-tuning conducted on LLaVA-1.5.
- Appendix C.2: we assess the performance of FTBI models without infusing any detection information, affirming that the FTBI fusion strategy proficiently harnesses the features extracted from ViT.
- Appendix C.3: we show the performance of FTBI models exclusively infusing OCR information or object detection information, affirming that they can respectively enhance the performance of our models on relevant tasks.
- Appendix C.4: we assess the inference efficiency of our models with detection information.

Appendix D, **Model Architecture Rationale:**

- Appendix D.1: we discuss how LLaVA-1.5 represents the majority of advanced MLLMs, and the results of LLaVA-1.5 can be extended to other MLLMs with similar structures. Additionally, we perform experiments on another MLLM, Qwen-VL, validating the versatility of our paper’s experimental findings.
- Appendix D.2: we show how do DINO and PaddleOCRv2 represent other detection models in our experiments. Additionally, we perform experiments on another detection model, YOLO-v8, validating that the specific format we devise for processing detection information to reduce the importance of model selection.
- Appendix D.3: we investigate other optional approaches to feed detection information into the LLM, comparing with our adopted text-based approach on the main page.

Appendix E, **Model Performance and Additional Evaluation Benchmarks:**

- Appendix E.1: we elaborate on the rationals to modify the GQA benchmark.
- Appendix E.2: we present benchmark scores for RBI models and FTBI models on MME-Perception and MME-Cognition.
- Appendix E.3: we evaluate our models’ ability to ground specific linguistic phenomena with the VALSE benchmark.
- Appendix E.4: we introduce weights to calculate the aggregated score based on the importance of each benchmark.

A More Demonstrative Examples

A.1 Examples on which LLaVA-1.5-13B fails while FTBI-13B with detection information succeeds.

Table 5 presents examples where LLaVA-1.5 provides incorrect responses, while our FTBI-13B delivers accurate answers. The showcased examples encompass scenarios related to object counting, object detection, and text recognition.

 <p>Q: How many breads are there in the picture?</p> <p>LLaVA-1.5-13B: There are three breads in the picture.</p> <p>FTBI-13B: There are four breads in the picture.</p>	 <p>Q: How many people are there in the image?</p> <p>LLaVA-1.5-13B: There are six people in the image.</p> <p>FTBI-13B: There are eight people in the image.</p>
 <p>Q: Count the number of sheep in this picture.</p> <p>LLaVA-1.5-13B: There are five sheep in this picture.</p> <p>FTBI-13B: There are six sheep in this picture.</p>	 <p>Q: What is the time in this picture?</p> <p>LLaVA-1.5-13B: The time in this picture is 12:00.</p> <p>FTBI-13B: The time in this picture is 11:10.</p>
 <p>Q: Are there potted plants? Where are them?</p> <p>LLaVA-1.5-13B: Yes, there are potted plants in the image. They are located on the floor, near the girl and the open closet.</p> <p>FTBI-13B: Yes, there are potted plants in the image. They are located on the left side of the room, near the bed.</p>	 <p>Q: What is written on the jersey of the player with number zero?</p> <p>LLaVA-1.5-13B: The jersey of the player with number zero reads "Stanford".</p> <p>FTBI-13B: The jersey of the player with number zero has "TITANS" written on it.</p>
 <p>Q: Find the person in the picture.</p> <p>LLaVA-1.5-13B: There is no person visible in the image. The scene shows a street with cars parked along the sidewalk, and a traffic light is present.</p> <p>FTBI-13B: There is a person standing on the sidewalk near the parked cars in the image.</p>	 <p>Q: What is the car number for the blue car?</p> <p>LLaVA-1.5-13B: The car number for the blue car is 547.</p> <p>FTBI-13B: The car number for the blue car is 87925.</p>

Figure 5: Examples on which LLaVA-1.5-13B fails while our model with detection information (FTBI-13B) succeeds.

A.2 Examples of Detection Information

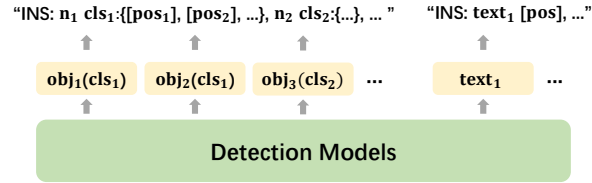


Figure 6: The composition of detection information. “INS”, “obj/cls” and “pos” indicate instruction, detected object/class name, and position text respectively.



Figure 7: Examples of detection information generated with DINO and PaddleOCRv2.

B Implementation Details

B.1 Length of Detection Information

Since the textual descriptions of bounding box coordinates typically involve a lot of digits, their token sequences are often long. As introduced in Section 3.2, we devise strategies to succinctly represent the spatial information of detected objects and texts, mitigating the verbosity of bounding box descriptions. By focusing on central coordinates and consolidating objects within the same category, we maintain brevity and clarity in our model’s inputs.

Table 6: The average sequence length of detection information.

	Average length	Average length (excluding 0)
Object Detection	118.5	125.1
OCR	29.4	97.5

We conduct a statistical analysis on the length of detection information using samples from the instruction-following dataset of LLaVA-1.5. According to the table, the average length of object detection information is 118.5, and the average length of OCR information is 29.4. After excluding the empty sequences, the average length of object detection information rises to 125.1, while the mean length of OCR information becomes 97.5. Consequently, these numbers fall in an acceptable range and will not excessively impact the efficiency of training and inference processes.

Additionally, it is observed that approximately 0.6% of object detection information exceeds a length of 512, whereas about 0.2% of OCR information surpasses the 512 threshold. In other words, our compression strategy has effectively mitigated the occurrence of lengthy sequences.

Finally, to ensure the length of the input sequence does not exceed the maximum context window length of LLM, we exclude object detection or OCR information that exceeds a length of 1,024.

B.2 LLaVA-1.5’s Instruction-following Dataset

The instruction-following dataset of LLaVA-1.5 [30] is a combination of several datasets that relate to various tasks. Among them, the LLaVA dataset [31] and ShareGPT dataset [7] comprise high-quality GPT-4 conversation data. VQAv2 [14] and GQA [18] present samples that require one word or a short phrase to answer visual questions. OKVQA [39] and A-OKVQA [44] are VQA datasets designed to expand the knowledge base of multimodal models through the incorporation of external prior knowledge. OCRVQA [40] is expressly tailored to enhance the text recognition capabilities of multimodal models. TextCaps [45] is an image captioning dataset, which presents samples in the form of concise one-sentence descriptions corresponding to images. RefCOCO [21] and VG [22] are object detection datasets designed to improve the object localization capabilities of multimodal models.

This dataset enables our models to better harness the additional detection information through the newly trained MLP and LoRA modules, especially with its object detection and OCR data.

Nevertheless, this dataset comprises only approximately 467K image samples, with only 116K designated for object detection and approximately 80K for text recognition, which is notably constrained. Consequently, should one seek to augment the model’s proficiency in assimilating detection information effectively, the exploration of dataset expansion emerges as a viable and recommended strategy.

Regarding the pretraining dataset of LLaVA-1.5, it is pertinent to note that this dataset predominantly consists of samples tailored for image captioning, thus inherently emphasizing image-level information. However, our detection information focuses more on fine-grained details, so we opt not to incorporate this dataset in our FTBI fusion strategy.

B.3 Image Resolution

The user-input images can be of any resolution and they are inputted into CLIP-ViT and detection modules respectively.

- For CLIP-ViT’s preprocessing, input images are processed to a size of 336x336 (requiring scaling and padding to form square images).
- For DINO and Grounding DINO’s preprocessing, input images can have arbitrary aspect ratios, but we need to limit the length of the shortest side to at least 224 and the length of the longest side to be within 2048. The setting for the shortest side length is to prevent insufficient multi-scale features extracted by DINO’s image encoder module, ensuring an adequate number of anchor boxes. The setting for the longest side length is to reduce additional memory usage, and this value can be set arbitrarily.
- For PaddleOCRv2, we can input images of any resolution and let the model process them autonomously.

B.4 Threshold Setting for Detection Models

We set certain thresholds for the detection models to reduce the acquisition of error information. Specifically, we set the threshold for DINO to 0.3 and only targets with confidence scores higher than this threshold are considered valid targets. For PaddleOCR, we set the detection box threshold to 0.6 and only detection boxes with confidence scores higher than this threshold are considered to contain text. For Grounding DINO, we set the detection box threshold to 0.35 and the text threshold to 0.25, and only targets meeting the requirements of both thresholds are considered valid targets.

B.5 Training Hyperparameters

In Table 7, we show the training hyperparameters employed in our experiments. These hyperparameters are derived from Vicuna [7] and LLaVA-1.5 [30] and have proven to be effective in our experiments. In the table, the term “Pretrain-RBI” denotes the hyperparameters used during the pretraining phase for vision-language alignment in RBI fusion strategy. “Finetune-RBI” refers to the hyperparameters employed for the subsequent fine-tuning phase focusing on visual instruction tuning in RBI fusion strategy. Additionally, “Finetune-FTBI” designates the hyperparameters used during the fine-tuning process for FTBI fusion strategy.

Table 7: Training hyperparameters of RBI and FTBI strategies.

Hyperparameter	Pretrain-RBI	Finetune-RBI	Finetune-FTBI
batch size	256	128	128
MLP lr	1e-3	2e-5	-
lr schedule		cosine decay	
lr warmup ratio		0.03	
weight decay		0	
optimizer		AdamW	
precision		bf16	
lora rank	-	128	128
lora alpha	-	256	256
lora lr	-	2e-4	2e-4

B.6 Time Consumption for Training

As for the experimental cost, on the 4xA100 (80G) platform, the pretraining process takes around 11 hours for 7B models and around 17 hours for 13B models. As for fine-tuning, it demands around 22 hours for 7B models and around 33 hours for 13B models.

C Further Experiments and Analysis on the FTBI Model

C.1 Fine-tuning on LLaVA-1.5 without Detection Information

Table 8: If we finetune LLaVA-1.5 without detection information, the performance will be inferior to the version with detection information. “-T w/o DI” stands for “training without detection information.”

MLLM	VQA ^{v2}	GQA*	VQA ^T	POPE	MME ^P	MME ^C	MMB	MMB ^{CN}	MM-Vet	SEED
FTBI-7B	79.0	80.1	60.1	88.9	1482.7	397.9	67.3	60.2	35.2	60.8
FTBI-7B-T w/o DI	78.2 ↓	79.0 ↓	58.2 ↓	86.8 ↓	1493.0 ↑	345.0 ↓	67.3	60.6 ↑	29.8 ↓	60.3 ↓
FTBI-13B	80.3	81.8	61.8	88.8	1555.1	365.4	71.4	65.2	38.9	62.3
FTBI-13B-T w/o DI	79.4 ↓	80.7 ↓	60.8 ↓	87.1 ↓	1509.0 ↓	315.4 ↓	71.0 ↓	63.9 ↓	36.1 ↓	62.8 ↑

In FTBI fusion strategy, our models undergo an additional epoch of fine-tuning on LLaVA-1.5. In the current experiment, we train a different version of our FTBI models without the infusion of detection information during training. In this way, we can investigate whether the performance improvement of our FTBI models is attributable to the supplementary detection information or to the fine-tuning of an additional epoch.

As indicated in Table 8, the performances of the models without detection information are on par with LLaVA-1.5. Compared to FTBI models, these models exhibit inferior performance across almost all benchmarks. Consequently, the outstanding performance of our FTBI models is more attributed to the detection information we supplement, rather than that we fine-tune for an extra epoch on LLaVA-1.5.

C.2 Analysis of FTBI Models without Detection Information

Table 9: If we do not infuse detection information to FTBI-7B during inference, its performance will be on par with LLaVA-1.5-7B. “w/o DI” is an abbreviation for “without detection information.”

MLLM	VQA ^{v2}	GQA*	VQA ^T	POPE	MME ^P	MME ^C	MMB	MMB ^{CN}	MM-Vet	SEED
LLaVA-1.5-7B	78.5	79.6	58.2	85.9	1510.7	355.7	64.3	58.3	30.5	58.6
RBI-7B w/o DI	76.4	74.8	56.6	85.5	1387.7	312.5	65.5	58.3	29.0	59.6
FTBI-7B w/o DI	78.0 ↑	78.4 ↑	57.1 ↑	86.0 ↑	1441.8 ↑	303.6 ↓	66.9 ↑	59.7 ↑	30.1 ↑	60.6 ↑
FTBI-7B	79.0	80.1	59.8	88.9	1482.7	397.9	67.3	60.2	35.2	60.8

Table 10: If we do not infuse detection information to FTBI-13B during inference, its performance will be on par with LLaVA-1.5-13B. “w/o DI” is an abbreviation for “without detection information.”

MLLM	VQA ^{v2}	GQA*	VQA ^T	POPE	MME ^P	MME ^C	MMB	MMB ^{CN}	MM-Vet	SEED
LLaVA-1.5-13B	80.0	81.0	61.3	85.9	1531.3	295.4	67.7	63.6	35.4	61.6
RBI-13B w/o DI	77.3	76.0	58.2	83.4	1442.6	310.7	68.5	61.7	30.6	61.6
FTBI-13B w/o DI	79.4 ↑	80.0 ↑	60.0 ↑	85.3 ↑	1525.7 ↑	320.0 ↑	70.8 ↑	64.8 ↑	36.0 ↑	61.7 ↑
FTBI-13B	80.3	81.8	61.8	88.8	1555.1	365.4	71.4	65.2	38.9	62.3

We assess the benchmark scores of FTBI models without infusing detection information to evaluate their capacities in leveraging ViT features. The findings delineated in Table 9 and Table 10 demonstrate that the efficacy of FTBI models without detection information aligns closely with that of LLaVA-1.5, and they outperform RBI models without detection information across all benchmarks. This implies that our third fusion strategy effectively empowers the model to assimilate and capitalize on information extracted by ViT.

C.3 Performance of FTBI Models Exclusively with OCR or Object Detection Information

As evident from Table 11 and Table 12, the inclusion of object detection information significantly boosts the scores of relevant benchmarks for object localization and object hallucination. Similarly, the incorporation of OCR information markedly improves the scores of benchmarks related to text recognition.

Table 11: Performance of FTBI models only with OCR information.

MLLM	VQA ^{v2}	GQA*	VQA ^T	POPE	MME ^P	MME ^C	MMB	MMB ^{CN}	MM-Vet	SEED
FTBI-7B w/o DI	78.0	78.4	57.1	86.0	1441.8	303.6	66.9	59.7	30.1	60.6
FTBI-7B-OCR	78.3 ↑	78.2	60.3 ↑	86.1	1454.4 ↑	399.3 ↑	66.7	59.5	35.1 ↑	60.5
FTBI-13B w/o DI	79.4	80.0	60.0	85.3	1525.7	320.0	70.9	64.8	36.0	61.7
FTBI-13B-OCR	79.7 ↑	80.0	61.8 ↑	85.4	1556.9 ↑	367.5 ↑	71.1	65.0	38.0 ↑	61.9

Table 12: Performance of FTBI models only with object detection information.

MLLM	VQA ^{v2}	GQA*	VQA ^T	POPE	MME ^P	MME ^C	MMB	MMB ^{CN}	MM-Vet	SEED
FTBI-7B w/o DI	78.0	78.4	57.1	86.0	1441.8	303.6	66.9	59.7	30.1	60.6
FTBI-7B-DINO	79.0 ↑	80.1 ↑	57.1	89.0 ↑	1469.2 ↑	302.1	67.2 ↑	60.2 ↑	31.5 ↑	61.0 ↑
FTBI-13B w/o DI	79.4	80.0	60.0	85.3	1525.7	320.0	70.9	64.8	36.0	61.7
FTBI-13B-DINO	80.0 ↑	81.8 ↑	60.1	89.0 ↑	1529.7 ↑	317.9	71.1 ↑	65.0 ↑	37.0 ↑	62.3 ↑

C.4 Inference Efficiency

We assess the time consumption of our FTBI-7B model by calculating its end-to-end inference time on the GQA and TextVQA datasets. When our model relies solely on object detection information during inference, DINO accounts for 38% of the total inference time. Additionally, when OCR information is exclusively infused, PaddleOCRv2 accounts for 25% of the total inference time. It is also noteworthy that, although the infusion of detection information incurs additional inference cost, as shown in Table 4, our model outperforms many state-of-the-art (SOTA) 13B or even larger multimodal large language models, which require considerably more resources. Moreover, thanks to the modularity and substitutability of our approach, a lighter and more efficient detection model could further improve the efficiency [49]. Additionally, since the embedded detection models are mutually independent, we can let them run independently on different devices, enabling parallel inference and further accelerating inference speed.

Regarding the proposed text compression strategy (Section 3.2), compared to using the original text output from detection models, the model with text compression achieves a 9% reduction in inference time when combined with object detection information, and a significant 58% reduction in inference time when combined with OCR information, verifying the effectiveness of the proposed strategy.

D Model Architecture Rationale

D.1 How LLaVA-1.5 Represents Other MLLMs?

In the main body of our paper, we exclusively select LLaVA-1.5¹ for experimentation, considering it representative of the majority of state-of-the-art models. In this section, we will illustrate this choice from the following two aspects:

(1) The representativeness of LLaVA-1.5. We choose LLaVA-1.5 as we are in a highly dynamic field and it is representative enough of most state-of-the-art MLLMs. The advanced MLLMs typically consist of three main modules: an image encoder, an input projector, and a LLM Backbone. LLaVA-1.5 adheres to this structure.

Images are first processed through the image encoder and the input projector. Most advanced MLLMs typically include a dedicated branch like this for processing image features into analogous image token sequences. Next, the image tokens are concatenated with text tokens that represent input sentences and fed into the LLM. Specifically, the text tokens representing our detection information can be directly concatenated with the extracted image tokens and used during MLLM’s training and inference. In other words, as long as the MLLM conforms to this structure, the additional detection information can be processed similarly before being inputted into the LLM, specifically being concatenated with image features at the embedding level. The way they are infused into the

¹We do not use LLaVA-1.6 (LLaVA-NeXT) in our experiments as it is concurrent to our work, and its training code is un-accessible until the NeurIPS submission deadline.

backbone LLM is similar. Therefore, the results of experiments conducted on LLaVA-1.5 can be applied to other MLLMs with similar structures.

Furthermore, LLaVA-1.5 has proven to be highly successful, spawning numerous outstanding works. We conduct our study based on LLaVA-1.5, enabling the application of our experimental findings to the subsequent works of LLaVA-1.5. Consequently, we are positioned to contribute to the open-source community.

(2) The empirical support on Qwen-VL. To better illustrate the versatility of our work, we also conduct experiments on another MLLM, Qwen-VL. Qwen-VL uses a cross-attention layer to compress visual features into a fixed-length sequence of 256, which differs from LLaVA-1.5’s MLP. And the datasets for training are also different.

Specifically, we conduct visual instruction tuning on Qwen-VL (which has not undergone visual instruction tuning) with the Instruction-following Dataset of LLaVA-1.5. We compare three models: Qwen-VL-IT, Qwen-VL-IT-TFI, and Qwen-VL-IT-RBI.

- **Qwen-VL-IT** refers to Qwen-VL undergoing regular visual instruction tuning. During the training and inference process, Qwen-VL-IT doesn’t incorporate detection modules.
- **Qwen-VL-IT-TFI** follows the same training process as Qwen-VL-IT, but it infuses detection information during inference, corresponding to the TFI fusion strategy in our paper.
- **Qwen-VL-IT-RBI** refers to fine-tuning Qwen-VL while simultaneously infusing detection information during training and inference, corresponding to the RBI fusion strategy in our paper (with a slight difference as it does not infuse detection information during the pretraining process).

We evaluate these models on 10 benchmarks, and the results are shown in Table 13.

Table 13: Comparison between “Qwen-VL-IT”, “Qwen-VL-IT-TFI”, and “Qwen-VL-IT-RBI”.

	VQA ^{v2}	GQA*	VQA ^T	MME ^P	MME ^C	POPE	MMB	MMB ^{CN}	MM-Vet	SEED
Qwen-VL-IT	79.4	77.8	49.9	1393.1	336.4	85.9	63.3	57.7	32.3	58.9
Qwen-VL-IT-TFI	78.1	80.9	49.7	1355.8	278.9	89.9	59.4	52.8	32.4	56.7
Qwen-VL-IT-RBI	78.9	82.2	54.4	1501.2	407.1	89.7	63.9	57.7	34.4	58.9

Based on Table 13, it is evident that the visual grounding capability of Qwen-VL-IT-TFI has improved compared to Qwen-VL-IT, resulting in significant score increases on the POPE benchmarks. However, Qwen-VL-IT-TFI exhibits varying degrees of decline in other tasks, similar to the results of TFI fusion strategy on the main page.

On the other hand, Qwen-VL-IT-RBI exhibits improvements across all benchmarks compared to both Qwen-VL-IT and Qwen-VL-IT-TFI, with notable score increases in both object detection and text recognition benchmarks. This mirrors the results of RBI fusion strategy on the main page, indicating that by infusing detection information during training, the model can better comprehend the detection information and consequently use it more effectively to address issues.

In summary, we elucidate the reasons behind LLaVA-1.5’s capability to serve as a representative model for many state-of-the-art MLLMs. We assert that the insights drawn from experiments on LLaVA-1.5 are broadly applicable to other structurally similar MLLMs. Furthermore, we conduct additional experiments on another MLLM, Qwen-VL, thereby demonstrating the extensive validity of our research findings.

D.2 How DINO and PaddleOCRv2 Represent Other Detecion Models?

Due to the specific textual format we designed for detection information, we can process the outputs of any object detection model and OCR model into detection information, as long as they can output the names of targets, the content of texts, and the corresponding coordinates of targets. (“*Here are the central coordinates of certain objects in this image: 2 people:[0.25, 0.12], [0.11, 0.43], 1 cake:[0.42, 0.32].*” or “*Here are the central coordinates of certain texts in this image: ‘Birthday’[0.41, 0.85], ‘YEARS’[0.11, 0.34].*”) In other words, the selection of object detection models and OCR models is not crucial. We only need to choose an excellent model based on performance and efficiency.

To better elucidate this point, we replace DINO with YOLOv8 and repeat the FTBI experiments, yielding the outcomes in Table 14.

Table 14: Comparison between “LLaVA-1.5-7B”, “FTBI-7B-DINO”, and “FTBI-7B-YOLOv8”.

	VQA ^{v2}	GQA*	VQA ^T	MME ^P	MME ^C	POPE	MMB	MMB ^{CN}	MM-Vet	SEED
LLaVA-1.5-7B	78.5	79.6	58.2	1510.7	355.7	85.9	64.3	58.3	30.5	58.6
FTBI-7B-DINO	79.0	80.1	59.8	1482.7	397.9	88.9	67.3	60.2	35.2	60.8
FTBI-7B-YOLOv8	78.6	80.4	59.9	1492.1	400.4	87.2	68.4	62.5	34.6	60.2

According to the table, both models bring similar performance improvements to the MLLM, suggesting that when the functionalities and performances of detection models are similar, their impact on the MLLM’s enhancement is also similar.

D.3 How Does Text-Based Detection Information Feeding Compare to Other Methods?

Besides the text-based approach, we conduct experiments on feeding the output vectors of DINO and PaddleOCRv2 into LLM, using either MLP layers or multiple cross-attention layers to map these vectors into LLM’s semantic space. However, these methods do not perform as well as the text-based approach. Below is the performance comparison among them, all of which are trained on 7B models using the RBI (Retraining Based Infusion) strategy.

Table 15: Comparison between the MLP approach, the cross-attention approach, and the text-based approach.

	VQA ^{v2}	VQA ^T	MME ^C	POPE
MLP	77.7	57.5	268.6	86.9
Cross-attention	77.2	57.4	265.4	85.9
Text-based	78.5	60.0	412.9	89.3

It can be observed that the performance improvements introduced by DINO and PaddleOCRv2 are not manifested in the MLP method and cross-attention method. We speculate that the occurrence of this phenomenon stems from insufficient training data, which is inadequate to train the newly initialized MLP module and cross-attention module. Unlike the outputs of CLIP-ViT, the output vectors of DINO and PaddleOCRv2 have not undergone contrastive learning with text, leading to significant discrepancies between these vectors and the text feature. Hence, more data is required to train the input projector effectively. However, introducing more data to train these newly introduced input projectors would render unfair performance comparisons with LLaVA-1.5.

Nevertheless, the text-based approach can effectively transmit the output information from DINO and PaddleOCRv2 to LLM without requiring additional training data. Therefore, we use the text-based approach.

E Model Performance and Additional Evaluation Benchmarks

E.1 Modification on the GQA Benchmark

In the original GQA benchmark, **a response is considered correct only when it precisely matches the reference answer**. However, due to the presence of numerous synonyms in the noun vocabulary, as well as variations in noun plurality, such evaluation criteria result in the omission of many correct responses. For example, if our model provides the response “ramp” instead of the expected answer “pavement”, or answers the question “What is the airplane flying above?” with “beach” instead of the expected answer “ocean”, it could lead to “inaccuracies”. Nonetheless, the model does not make mistakes.

Thus, we make modifications to the GQA benchmark. We select only a subset of the evaluation dataset, including samples that only require yes or no answers, as well as those involving choices (questions containing “or”). For these samples, their correct answers can be chosen from a limited

set of options, eliminating the possibility of evaluated models providing correct but non-matching answers, which leads to more accurate evaluation outcomes. After filtering, the remaining number of samples is 5,677, approximately half of the original evaluation dataset. We name the modified evaluation benchmark as GQA*.

E.2 MME Benchmark in Table 4

Table 16: Comparison of SOTA MLLMs on the MME benchmark.

MLLM	MME-Perception	MME-Cognition
BLIP-2	1293.8	290.0
InstructBLIP	1212.8	291.8
Qwen-vl	1400.6	266.4
Qwen-VL-Chat	1487.5	360.7
SPHINX	1476.1	322.2
LLaVA-1.5-7B	1510.7	355.7
RBI-7B	1454.5	412.0
FTBI-7B	1482.7	397.9
LLaVA-1.5-13B	<u>1531.3</u>	295.4
RBI-13B	1491.2	<u>409.6</u>
FTBI-13B	1555.1	365.4

In Table 16, we present benchmark scores for RBI models and FTBI models on MME-Perception and MME-Cognition. The value reveals a significant enhancement in scores for both models specifically on MME-Cognition. This notable enhancement can be ascribed to the inclusion of supplementary OCR information, addressing a multitude of questions within MME-Cognition that pertain to textual content embedded within images.

Furthermore, concerning the MME-Perception benchmark, our models exhibit some fluctuations in scores. Nonetheless, it is noteworthy that the scores for FTBI models surpass those for RBI models, which underscores that our third fusion approach better preserves the original capabilities of MLLM.

E.3 Performance on the VALSE Benchmark

VALSE[41](Vision And Language Structured Evaluation) is a zero-shot benchmark designed to test the visual-linguistic grounding capabilities of general-purpose pre-trained vision-language models on specific linguistic phenomena. It can assess many capabilities of MLLMs, including six aspects: existence, plurality, counting, spatial relations, actions, and entity co-reference.

In VALSE, a valid instance consists of an image, a caption, and a modified caption called a ‘foil’ that exemplifies a specific linguistic phenomenon. The tested model is required to distinguish between real captions and foils. VALSE employs four metrics to evaluate the model’s performance: overall accuracy (acc) on all classes (foil and correct); precision (p_c) measuring how well models identify the correct examples; foil precision (p_f) measuring how well foiled cases are identified; and pairwise ranking accuracy (acc_r), which measures whether the image-sentence alignment score is greater for a correct image-text pair than for its foiled pair. acc_r is more permissive than acc as it accepts model predictions if the score for a foil is lower than the caption’s score.

Due to the inability of LLaVA-1.5 and our models to directly output “cross_relationship_score” as the image-sentence alignment score like models such as LXMERT, we modify the computation of acc_r , acc , p_c and p_f following the approach outlined in “lxmert_valse_eval.py” (https://github.com/Heidelberg-NLP/VALSE/blob/main/lxmert_valse_eval.py) as follows:

(1) Let the model answer the following two questions and tally the number of ‘yes’ and ‘no’ responses for each question.:

- Q1: “Does this image match the sentence ‘caption’? Use only ‘yes’ or ‘no’ to answer.”
- Q2: “Does this image match the sentence ‘foil’? Use only ‘yes’ or ‘no’ to answer.”

(2) When the answer to Question 1 is “yes”, increment the counters for *foil_accuracy* and *capt_fits*. When the answer to Question 2 is “no”, increment the counters for *foil_detected* and *foil_accuracy*. If the answer to Question 1 is “yes” and the answer to Question 2 is “no”, increment the counter for *pairwise_acc*.

(3) The final calculation formula is:

$$acc = \frac{foil_accuracy}{count} * 50,$$

$$p_c = \frac{capt_fits}{count} * 100,$$

$$p_f = \frac{foil_detected}{count} * 100,$$

$$acc_r = \frac{pairwise_acc}{count} * 100$$

Table 17: Comparison between FTBI-7B and LLaVA-1.5-7B on the VALSE benchmark.

		Existence	Plurality	Counting_hard	Counting_small
acc_r	LLaVA-v1.5-7B	69.9	13.4	35.9	35.6
	FTBI-7b	70.5	17.6	46.1	51.6
acc	LLaVA-v1.5-7B	84.0	56.2	64.6	66.9
	FTBI-7b	84.1	58.1	71.1	74.4
$min(p_c, p_f)$	LLaVA-v1.5-7B	73.7	16.0	52.1	45.7
	FTBI-7b	71.5	22.1	69.5	65.3
		Counting_adversarial	Relations	Action Replacement	Actant Swap
acc_r	LLaVA-v1.5-7B	25.2	4.7	34.3	10.3
	FTBI-7b	36.3	8.2	37.4	19.2
acc	LLaVA-v1.5-7B	55.6	52.0	66.4	53.1
	FTBI-7b	64.8	53.4	67.6	57.3
$min(p_c, p_f)$	LLaVA-v1.5-7B	39.8	7.5	43.8	16.7
	FTBI-7b	59.5	14.6	52.9	30.2
		Coreference	Coreference_hard	Foil_it	
acc_r	LLaVA-v1.5-7B	5.2	4.8	50.5	
	FTBI-7b	20.2	18.3	63.0	
acc	LLaVA-v1.5-7B	52.3	52.4	75.1	
	FTBI-7b	58.6	55.8	81.4	
$min(p_c, p_f)$	LLaVA-v1.5-7B	6.4	4.8	53.5	
	FTBI-7b	24.0	20.2	66.6	

The results are presented in Table 17. It can be observed that FTBI-7B outperforms LLaVA-v1.5-7B in all aspects, which indicates that our model is more sensitive to foiled instances and has better capabilities in visual grounding. It also emphasizes that the incorporation of the object detection module has indeed enhanced the object detection proficiency of the MLLM.

E.4 Applying Weights on the Aggregated Score

The purpose of introducing the aggregated score is to provide a rough comparison of our models’ overall performance with other MLLMs, especially LLaVA-1.5. In our analysis, we don’t place too much emphasis on the comparison of this aggregated score. Instead, we focus more on comparing individual benchmarks and analyzing the performance changes of our models.

It’s possible for the aggregated score to introduce unfairness due to the varying significance of different benchmarks. To enhance fairness, we introduce weights to calculate the aggregated score based on the importance of each benchmark. Specifically, we assign weights of 0.5 or 0 to less significant benchmarks MM-Bench and Seed-Bench, while setting the weights of other benchmarks to 1.

Table 18: The aggregated score with different weights.

	<i>Weight = 0.5</i>	<i>Weight = 0</i>
InstructBLIP	0.285	0.345
Qwen-VL	0.574	0.668
Qwen-VL-Chat	0.765	0.778
SPHINX	0.713	0.665
LLaVA-1.5-7B	0.769	0.771
RBI-7B (ours)	0.830	0.832
FTBI-7B (ours)	0.870	0.882
LLaVA-1.5-13B	0.839	0.834
RBI-13B (ours)	<u>0.896</u>	<u>0.898</u>
FTBI-13B (ours)	0.946	0.954

According to Table 18, with the introduction of low weights for less significant benchmarks, our models still exhibit higher scores, demonstrating superior overall performance.